© 2016. Published by The Company of Biologists Ltd | Journal of Cell Science (2016) 129, 2250-2260 doi:10.1242/jcs.182592

RESEARCH ARTICLE

Innervation regulates synaptic ribbons in lateral line mechanosensory hair cells

Arminda Suli[1,2,*], Remy Pujol[3,4], Dale E. Cunningham[3], Dale W. Hailey[2,3], Andrew Prendergast[2,5], Edwin W. Rubel[3] and David W. Raible[2]

ABSTRACT

Failure to form proper synapses in mechanosensory hair cells, the sensory cells responsible for hearing and balance, leads to deafness and balance disorders. Ribbons are electron-dense structures that tether synaptic vesicles to the presynaptic zone of mechanosensory hair cells where they are juxtaposed with the post-synaptic endings of afferent fibers. They are initially formed throughout the cytoplasm, and, as cells mature, ribbons translocate to the basolateral membrane of hair cells to form functional synapses. We have examined the effect of post-synaptic elements on ribbon formation and maintenance in the zebrafish lateral line system by observing mutants that lack hair cell innervation, wild-type larvae whose nerves have been transected and ribbons in regenerating hair cells. Our results demonstrate that innervation is not required for initial ribbon formation but suggest that it is crucial for regulating the number, size and localization of ribbons in maturing hair cells, and for ribbon maintenance at the mature synapse.

KEY WORDS: Ribbon synapse, Mechanosensory hair cells, Innervation, Zebrafish, *Neurogenin 1*, *Sputnik*

INTRODUCTION

Ribbons (also known as dense bodies) are electron-dense structures that tether glutamate-containing synaptic vesicles and are found at synapses of sensory cells that respond to a broad range of stimulus intensities, such as mechanosensory hair cells of the auditory and lateral line system (in fish and amphibians), retinal photoreceptor and bipolar cells, and pineal cells (reviewed in Moser et al., 2006; Nouvian et al., 2006; Matthews and Fuchs, 2010; Yu and Goodrich, 2014; Nicolson, 2015). They are thought to store a ready-releasable pool of synaptic vesicles and coordinate synchronous vesicle-release at the synapse (Khimich et al., 2005; Buran et al., 2010; Matthews and Fuchs, 2010; Maxeiner et al., 2016). Voltage gated L-type Ca^{2+} channels are found to drive exocytosis at ribbon synapses and are localized at the base of ribbons (Platzer et al., 2000; Brandt et al., 2003; Dou et al., 2004; Sidi et al., 2004; Sheets et al., 2012; Wong et al., 2014). In zebrafish, these channels are also found to play a role in regulating ribbon size, number and maintenance of ribbons at the hair cell synapse (Sheets et al., 2012). Failure to properly form and localize ribbons at the synapse leads to impaired synaptic transmission and sensory input propagation. Mice defective for bassoon, a cytomatrix protein thought to anchor ribbons at the synapse, show reduced exocytosis in auditory mechanosensory hair cells, reduced reliability of spiking at the auditory stimulus onset, abnormal auditory brain responses and lower amplitudes of b-wave responses during electroretinographic recordings in the eye (Brandstatter et al., 1999; Dick et al., 2003; Khimich et al., 2005; tom Dieck et al., 2005; Buran et al., 2010). Zebrafish larvae in which *ribeye b*, a gene coding for a major scaffolding protein in synaptic ribbons (Schmitz et al., 2000; Zenisek et al., 2004; Wan et al., 2005; Magupalli et al., 2008), is knocked down show reduction in the number of spikes of afferent neurons of the lateral line mechanosensory hair cells when the hair cells are stimulated (Sheets et al., 2011). Similarly, knockout mice for the ribeye gene (also known as *Ctbp2*) show impaired neurotransmitter release at retinal bipolar cells (Maxeiner et al., 2016).

Electron microscopy and immunohistochemistry data shows that ribbon size and localization changes during cell development and the establishment of functional synapses. During early development of auditory hair cells and retinal photoreceptor cells, electron-dense ribbon precursors are found apically in the cytoplasm (Blanks et al., 1974; Sobkowicz et al., 1982, 1986; Regus-Leidig et al., 2009; Sheets et al., 2011; Wong et al., 2014). These cytoplasmic ribbon precursors in retinal photoreceptor cells colocalize with the cytomatrix proteins bassoon and piccolo and are thought to be shuttled together to the active zone (Regus-Leidig et al., 2009). As synaptogenesis proceeds, the total number of ribbons decreases, ribbons become localized at the active zone and fewer ribbon precursors are found in the cytoplasm. Whereas multiple ribbons are found at the site of immature hair cell synapses, mature synapses have single ribbons (Pujol et al., 1979; Sobkowicz et al., 1986; Pujol et al., 1997; Wong et al., 2014).

To date, few studies have looked at the role that innervation has on ribbon placement and maintenance at the active zone. Sobkowicz and colleagues have shown by electron microscopy that when compared to their innervated counterparts, inner hair cells in denervated cultured mouse cochlea have a higher percentage of ribbons misplaced from the synapse, even though they maintain their engagement with the hair cell membrane (Sobkowicz et al., 1986). Similarly, ribbons are found in positions other than the synapse in cochlear hair cells of guinea pigs after the post-synaptic fibers are damaged following intracochlear perfusion with 200 µM AMPA (Puel et al., 1995). Furthermore, the number of hair cell ribbons, as assessed by immunohistochemistry, is decreased in brain-derived neurotrophic factor (BDNF)- or Mafb-knockout postnatal mice, where innervation is reduced or delayed (Zuccotti et al., 2012; Yu et al., 2013), and in adult mice when ouabain is applied in the round window causing de-afferentation of cochlear hair cells (Yuan and Chi, 2014). Although these observations were

[1]Department of Physiology and Developmental Biology, Brigham Young University, Provo, UT 84602, USA. [2]Department of Biological Structure, University of Washington, Seattle, WA 98195, USA. [3]V.M. Bloedel Hearing Center, University of Washington, Seattle, WA 98195, USA. [4]INSERM-Unit 1051, Université Montpellier, France. [5]Institut du Cerveau et de la Moelle Épinère 47, Boulevard de l'Hôpital, 75013 Paris, France.

*Author for correspondence (asuli@byu.edu)

A.S., 0000-0003-2690-8407

Received 4 November 2015; Accepted 15 April 2016

Journal of Cell Science (2016) 129, 2250-2260 doi:10.1242/jcs.182592

made either with *in vitro* preparations, such as the cultured cochlea, or in conditions which might affect both the nerve and the hair cells, such as in BDNF mutants and in treated cochlea, these studies suggest that innervation is required for localizing ribbons at the synapse and regulating their number in mechanosensory hair cells.

To directly investigate how innervation affects ribbon formation in an *in vivo* model, we used the zebrafish mechanosensory lateral line system. Because of the ability to generate mutants through forward genetic screens in zebrafish and the accessibility of lateral line hair cells, this system has become valuable in discovering the molecular mechanisms that oversee hair cell development and ribbon synapse formation (Nicolson et al., 1998; Nicolson, 2005, 2015).

The mechanosensory lateral line system is an additional sensory system found in fish and amphibians (Dijkgraaf, 1963, 1989). It measures constant input from water vibrations and is used in part to detect prey and predators, and orient fish in water currents (Hoekstra and Janssen, 1985; Blaxter and Fuiman, 1989; Hassan, 1989; Montgomery et al., 1997; Montgomery and Hamilton, 1997; Baker and Montgomery, 1999; Kanter and Coombs, 2003; Suli et al., 2012). In zebrafish, the sensory organs, called neuromasts, develop in stereotypical positions along the body and are located exclusively on the body surface of developing larvae; in adults they are found both on the body surface and within bony canals (Raible and Kruse, 2000; Webb and Shirey, 2003; Ghysen and Dambly-Chaudiere, 2007). Neuromasts are comprised of support cells and mechanosensory hair cells, which are similar in characteristics and function to auditory and vestibular hair cells (Kalmijn, 1989). To determine the role of innervation in hair cell ribbon synapses, we analyzed mutants that lack innervation, removed hair cell innervation by cutting innervating fibers after synaptogenesis and looked at ribbon formation during hair cell regeneration.

RESULTS

Ribbons in mechanosensory lateral line hair cells during development

The shape and size of ribbons differ across cell types, developmental stages and species (reviewed in Sterling and Matthews, 2005; Moser et al., 2006; Nouvian et al., 2006). In all cell types, ribbon precursors initially appear as spheres; however, as ribbons mature, in some cell types, their shape changes. For example, in mature auditory hair cells ribbons are ellipsoid, whereas in mature photoreceptor cells they appear as sheets (Sterling and Matthews, 2005; Nouvian et al., 2006). Transmission electron microscopy (TEM) shows that in mature zebrafish mechanosensory lateral line hair cells, ribbons at the synapse are spherical with a diameter of about 300 nm (Sidi et al., 2004; Obholzer et al., 2008; Nicolson, 2015) (Fig. 1A). To determine whether ribbon size at the synapse differs with hair cell maturation, we fixed and stained 2 days post fertilization (dpf) embryos to 7 dpf larvae for TEM and imaged ribbons in hair cells. We found that ribbons at the synapse remained spherical during development. Their diameter as calculated by averaging measurements obtained in two planes, one perpendicular to the active zone and the other horizontal to the active zone, was ~300 nm (Fig. 1B). There is a slight size difference between ribbons at 3 dpf and 4 dpf, which might be indicative of ribbon maturation during hair cell development.

Innervation is important for ribbon regulation in mechanosensory hair cells

Mechanosensory hair cells of the lateral line are innervated by lateral line ganglion neurons that project afferent fibers to hair cells and octavolateralis efferent neurons that provide cholinergic input to hair cells. To initially address the requirement of innervation in ribbon formation, we analyzed ribbons in lateral line hair cells of *neurogenin1* mutants (*neurog1*) (Golling et al., 2002; McGraw et al., 2008), given that *neurog1* knockdown results in a lack of afferent innervation of hair cells (Grant et al., 2005). Antibody staining for acetylated tubulin confirmed that *neurog1* mutants lack afferent innervation of the posterior lateral line neuromasts (Fig. 2A,B). However, we further observed that the afferent innervation of the anterior lateral line neuromasts was not affected in these mutants, suggesting that *neurog1* is only required in the development of the posterior lateral line ganglion and not the anterior lateral line ganglion. When we stained with the SV2 antibody, which recognizes efferent fibers, we similarly found that *neurog1* mutants lack efferent innervation in the posterior lateral line (data not shown) but not the anterior lateral line. Therefore, hair cells in posterior lateral line neuromasts cannot send input to the central nervous system through afferent fibers, and are devoid of efferent input from the octavolateralis efferent neurons. We assessed the role of innervation in ribbon formation by looking at ribbons in these non-innervated posterior lateral line hair cells (Fig. 2D,D′,F,F′) and comparing them to their wild-type siblings

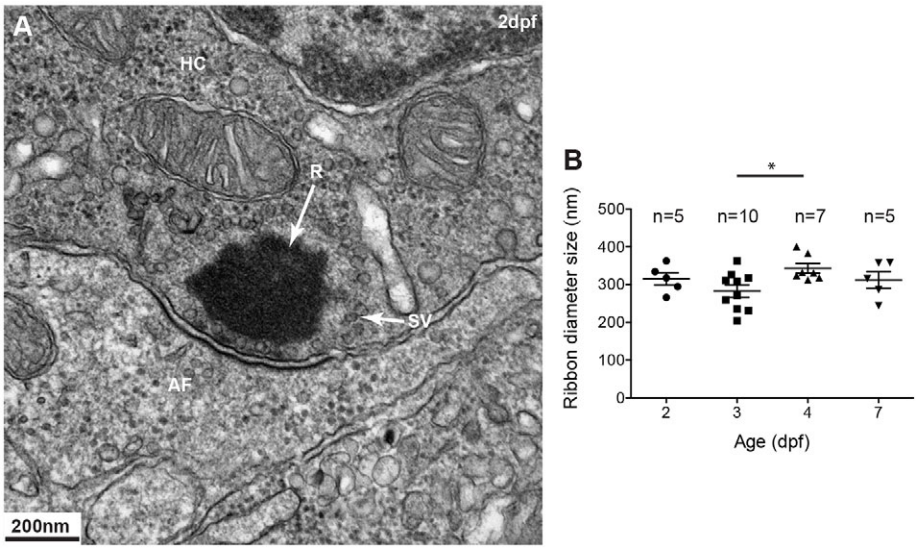

Fig. 1. Ribbons in mechanosensory lateral line hair cells. (A) Transmission electron micrograph (TEM) of a typical spherical ribbon (R) in a mechanosensory hair cell (HC) from a lateral line neuromast in zebrafish. Ribbons are electron-dense structures, anchored to the presynaptic membrane, that tether synaptic vesicles (SV) at synapses with afferent fibers (AF). Vesicles ready to be docked are at the membrane facing the post-synaptic membrane density. (B) At different stages during development, from 2–5 days post fertilization (dpf), ribbons at the synapse measure ~300 nm in diameter. A one-way ANOVA shows no significant difference (R^2=0.2552, P=0.7560); a Tukey's multiple-comparison test shows a significant difference only between day 3 and 4 ribbons (*P<0.05). Results are mean±s.e.m.

Journal of Cell Science (2016) 129, 2250-2260 doi:10.1242/jcs.182592

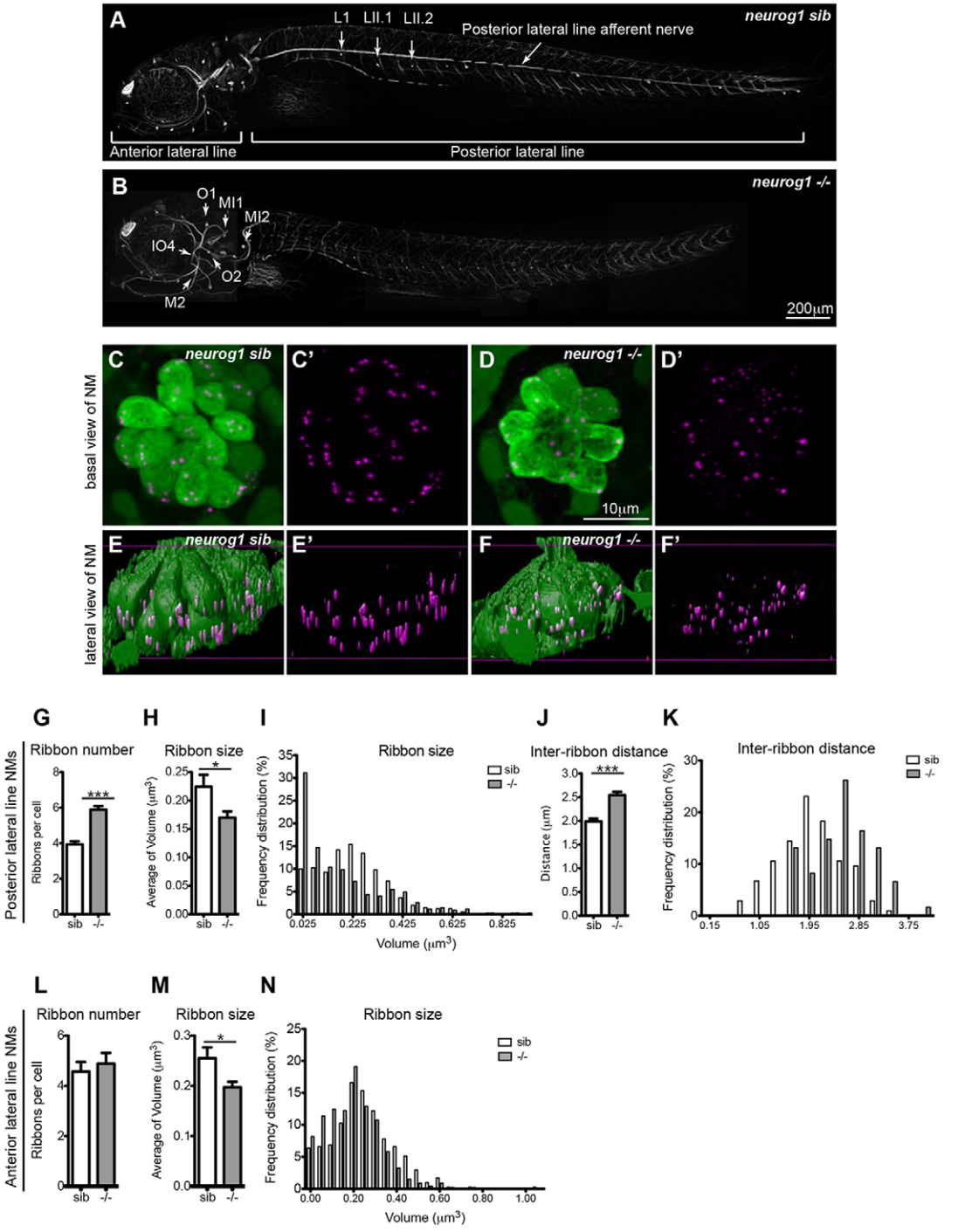

Fig. 2. Innervation is required for regulation of ribbon size, number and localization. (A,B) Afferent innervation in neurogenin (*neurog1*) siblings (sib) (A) and mutants (–/–) (B) as detected by antibody staining for acetylated tubulin. *neurog1* mutants (B) lack afferent and efferent (data not shown) innervation of posterior lateral line hair cells but not anterior lateral line hair cells. A total of nine neuromasts (NM) per condition were used for confocal microscopy imaging and ribbon analysis: three posterior lateral line neuromasts (L1, LII.1, LII2) and three anterior lateral line neuromasts (O2, MI1, MI2, IO4 or M2) per larvae were measured in three different larvae. (C–D′) Projections of confocal images of the posterior lateral line neuromasts immunolabeled to show hair cells (green, anti-parvalbumin antibody) and ribbons (magenta, anti-RibeyeB antibody). (E–F′) Lateral views of surface renderings of neuromasts in C–D′ generated by Huygens software. Ribbon size, number and inter-ribbon distance were obtained from the surface renderings of the neuromasts (see Materials and Methods). In *neurog1* siblings, ribbons were found at the base of hair cells (E,E′), whereas in *neurog1* mutants, ribbons were found both in the cytoplasm and at the base of posterior lateral line hair cells (F,F′). Additionally, in *neurog1* mutants, ribbons were fewer in number (G), smaller in average size (H,I) and the distance between ribbons was also increased (J,K). The number of ribbons per cell in anterior lateral line hair cells, which are innervated, did not differ between *neurog1* mutants and sibling larvae (L) but ribbon size was smaller in *neurog1* mutant hair cells (M). Ribbon size and number were obtained from the surface renderings of the neuromasts (see Materials and Methods). **P*=0.09 in H, **P*=0.03 in M, ****P*<0.0001. Statistical analysis of ribbons (unpaired two tailed *t*-test) was performed on averages of averages – we calculated the average of ribbons per cell in a given neuromast and then averaged this number across nine total neuromasts (three neuromasts in three different larvae). Posterior lateral line neuromasts in *neurog1* mutants had an average of nine hair cells per neuromast, whereas anterior lateral line neuromasts had an average of 11 hair cells per neuromast. Posterior lateral line neuromasts in *neurog1* siblings had an average of 12 hair cells per neuromast, whereas anterior lateral line neuromasts had an average of 10 hair cells per neuromast. Results are mean±s.e.m.

Journal of Cell Science (2016) 129, 2250-2260 doi:10.1242/jcs.182592

(Fig. 2C,C′,E,E′). Confocal microscopy on *neurog1* mutants stained with an antibody against RibeyeB (Sheets et al., 2011), a scaffolding protein that is part of ribbons, showed that ribbons are present in *neurog1*$^{-/-}$ posterior lateral line hair cells (Fig. 2D′,F′) suggesting that ribbon formation is an intrinsic function of the hair cells rather than a response to innervation. Even though ribbons formed in *neurog1*$^{-/-}$ hair cells at 5 dpf, their placement in the cell was different from that in wild-type animals. In mutant cells, devoid of afferent and efferent innervation, ribbons were both adjacent to the basal membrane and distal from it (Fig. 2F′). Although we were not able to quantify this effect, the difference is qualitatively evident in the images in Movie 1 (*neurog1*$^{-/-}$) and Movie 2 (*neurog1* sibling). When we measured the distance between individual ribbons within a cell (inter-ribbon distance), we found that it was increased in *neurog1*$^{-/-}$ posterior lateral line hair cells (Fig. 2J,K). Additionally, we noticed that ribbon number was increased in *neurog1*$^{-/-}$ hair cells and that ribbon size distribution was different from in their siblings, with *neurog1*$^{-/-}$ hair cells showing an increase in smaller-size ribbons (Fig. 2G,I). We also calculated the average size of ribbons, which appeared reduced in *neurog1*$^{-/-}$ hair cells (Fig. 2H). We recognize that we are at the limit of resolution with light microscopy, and thus ribbon sizes are semi-quantitative and might not reflect the true size of ribbons. By contrast, the anterior lateral line hair cells in *neurog1*$^{-/-}$, which retain innervation, showed no difference in ribbon number (Fig. 2L) and a similar ribbon size distribution (Fig. 2N), although the average ribbon size was smaller when compared to their siblings (Fig. 2M). When assessed by TEM, ribbons in 5 dpf posterior lateral line hair cells of *neurog1*$^{-/-}$ mutants were not tethered at the membrane (Fig. 3A′,B). From our observations of neuromasts in four different larvae, we found five cases of such ribbons. In addition, in mutant hair cells there appeared to be many more vesicles than in wild-type cells (Fig. 3C). Although we did not perform true serial sectioning (on formvar-coated grids), we followed the same ribbon across three to five ~90 nm sections to determine the presence of attachments at the membrane. Representative micrographs are shown in Fig. 3A′,B. Taken together, our data demonstrate that innervation is not important for initial generation of ribbons, but suggest that it is crucial for their correct localization at the plasma membrane and for the regulation of ribbon number and size.

Innervation is required for maintenance of ribbons at the membrane

Although, initial ribbon formation appears to be an intrinsic property of the hair cell, the question arises as to whether innervation is necessary for subsequent ribbon maintenance at the membrane. To address this issue, we transected the posterior lateral line nerve anterior to the L1 neuromast on one side of 5 dpf larvae (a stage after synapses are established) by applying three iterations of 5-ms 532-nm laser pulses using a spinning disc confocal microscope (Fig. 4A,B). For these experiments, we used *Tg(neuroD:GFP)* larvae (Obholzer et al., 2008), whose GFP-labeled lateral line ganglion neurons allow visualization of afferent fibers. Because efferent fibers use afferents to pathfind during development and maintain a close proximity at later stages (data not shown), we were unable to affect afferent or efferent fibers separately; therefore, hair cells in the transected side lacked both afferent and efferent innervation. At 24 h after neuronal fiber transection, we immunostained with the anti-RibeyeB antibody and compared the ribbons in denervated posterior lateral line hair cells (Fig. 4B) to the ribbons in the non-transected control side (Fig. 4A). In the control side, ribbons remained adjacent to the membrane (Fig. 4E′), whereas in the denervated hair cells, ribbons were found both adjacent to the basolateral membrane and distal to it (Fig. 4F′), similar to those in *neurog1* mutants. Furthermore, the number of ribbons in denervated hair cells was higher than in controls

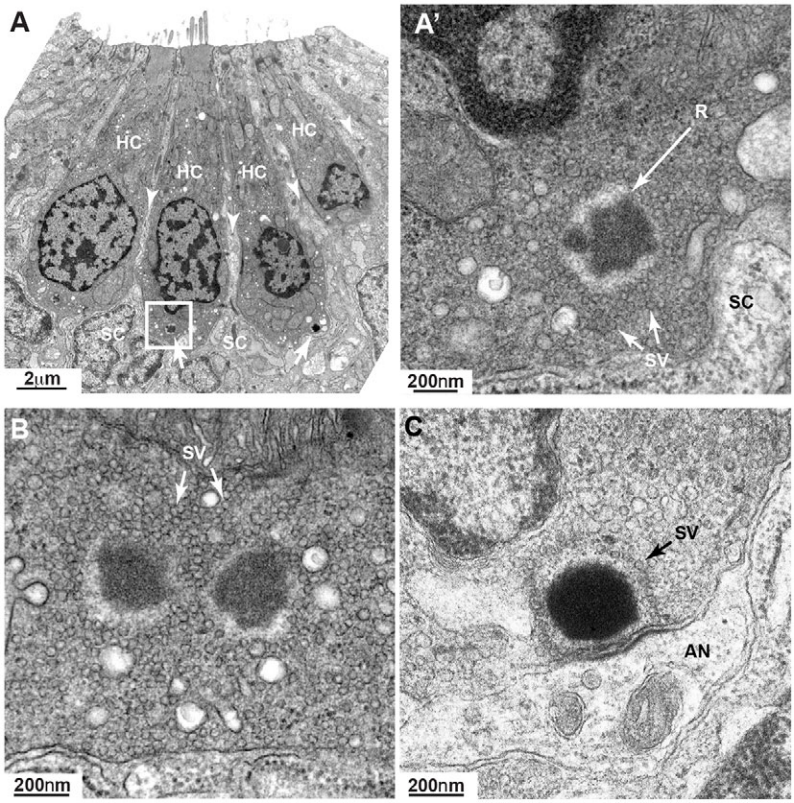

Fig. 3. Ribbons in *neurog1* mutants are cytoplasmic and show an increased pool of synaptic vesicles. (A) TEM transverse section of a posterior lateral line neuromast showing four mature hair cells (HC) surrounded by clearer cytoplasm (arrowheads) of support cells (SC). Even at this low magnification, two ribbons (arrows) are clearly seen. The ribbon in the inset is enlarged in A′ showing more clearly its ectopic position (not anchored at membrane) and a greater amount of surrounding synaptic vesicles (SV) not tethered to the ribbon (R). At the basal pole of the hair cell only the clear cytoplasm of the support cell can be seen. (B) A hair cell from another neuromast shows a double-ribbon, also ectopic, with a profusion of untethered SVs. (C) A ribbon in a wild-type 7 dpf hair cell is shown for comparison. A monolayer of SVs surrounds the ribbon. AN, afferent neuron.

Journal of Cell Science (2016) 129, 2250-2260 doi:10.1242/jcs.182592

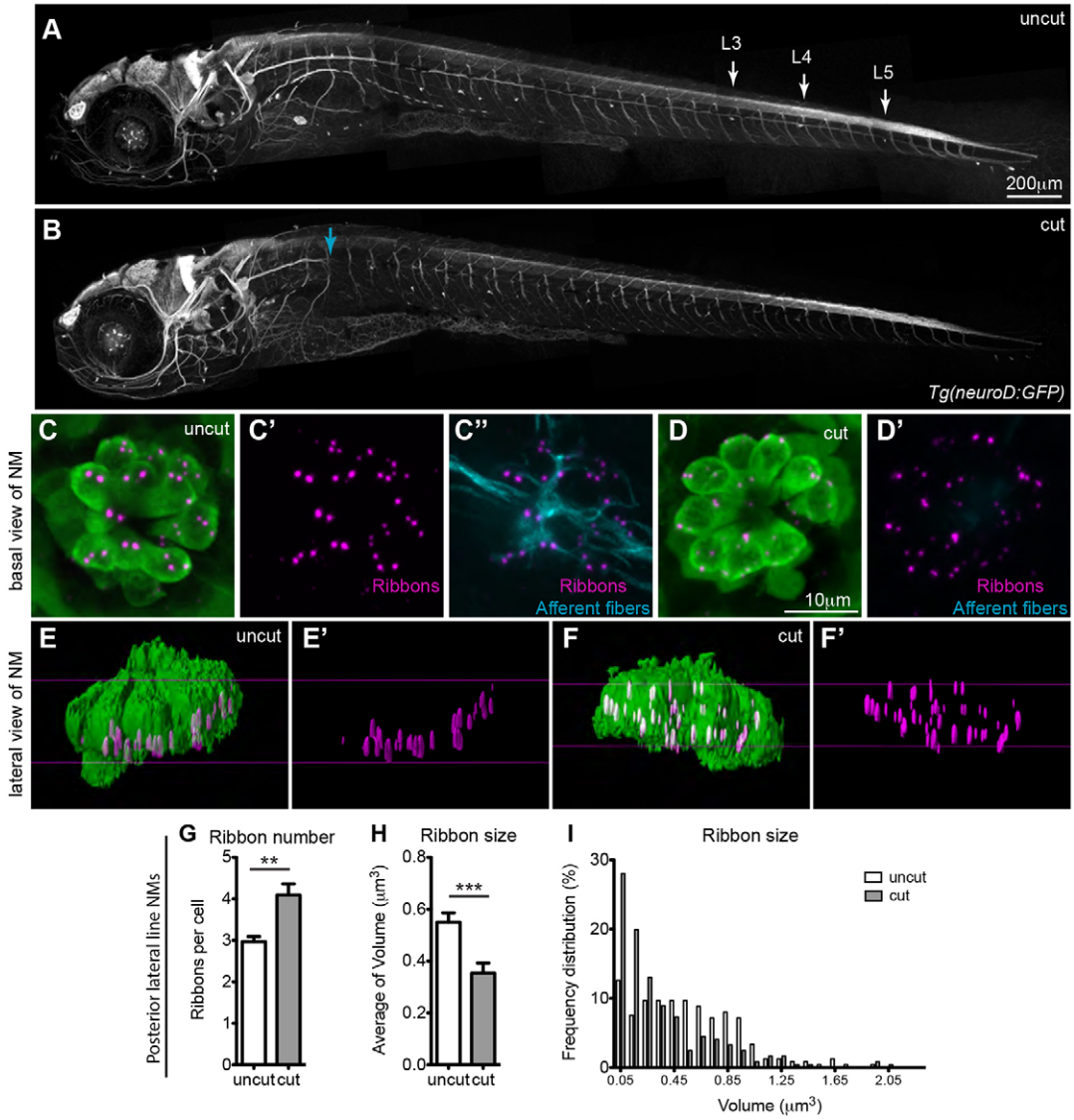

Fig. 4. Continuous innervation is required for regulating ribbons in hair cells. Ribbon number and size was assayed in 5 dpf larvae with mature neuromast hair cells, whose lateral line fibers were transected on one side of the larva, after the nerves had formed synapses with hair cells. *Tg(neuroD:GFP)* transgenic animals were used to visualize lateral line afferent fibers *in vivo* before and after transection. (A) Lateral line afferents in the uncut side of the larva as visualized by acetylated tubulin staining. (B) Lateral line afferents transected (cut) at the level of L1 neuromast in the opposite side of the larva (blue arrow). Cut and uncut larvae were fixed at 24 h post transfection and stained for hair cells (green, anti-parvalbumin antibody), ribbons (magenta, anti-RibeyeB antibody) and afferent neurons (cyan, anti-GFP antibody). Projections of confocal microscope images of the uncut (C–C″) and cut (D,D′) side were acquired at the level of L3, L4 and L5 neuromasts (NM) in the posterior lateral line (A). The absence of afferent fibers in neuromasts of the cut side is seen in D′, which is an overlay of RibeyeB (magenta) and anti-GFP antibody staining (no cyan staining was present), whereas neuromasts in the uncut side continue to be innervated by afferent fibers (C″). (E–F′) Lateral views of surface renderings of neuromasts in C–D′ generated by Huygens software. In the denervated hair cell, the number of ribbons/cell increased (G), whereas the size of ribbons decreased (H,I). Ribbon size and number were obtained from the surface renderings of the neuromasts (see Materials and Methods). $^{**}P$=0.0036, $^{***}P$=0.0006. Statistical analysis of ribbons (unpaired two tailed *t*-test) was performed on averages of averages – we calculated the average of ribbons per cell in a given neuromast and then averaged this number across six total neuromasts (three neuromasts in two different larvae). Posterior lateral line neuromasts had an average of 10 hair cells per neuromast in cut larvae and an average of 13 hair cells/neuromast in uncut larvae. Results are mean±s.e.m.

(Fig. 4G), and there was a higher percentage of smaller-size ribbons (Fig. 4H,I). These data demonstrate that innervation is not only important for regulating ribbon localization, size and number, but that continuous innervation influences ribbon maintenance and stability.

Innervation leads to ribbon stabilization in regenerating hair cells

To follow ribbon dynamics as hair cells mature and establish synapses, we looked at ribbons during hair cell regeneration. Because they are localized on the surface of zebrafish larvae, lateral line hair cells are susceptible to mechanically or pharmacologically induced cell death, but can overcome such insults by promptly regenerating (Harris et al., 2003). Following hair cell death, the afferent innervating fibers remained proximal to the neuromasts (Fig. S1, Movie 3, wild-type; Movie 4, after hair cell death). We incubated 5 dpf zebrafish larvae for 1 h with 400 μM neomycin to kill hair cells, fixed the larvae at different time points during regeneration, and processed samples both for immunohistochemistry and TEM. Looking at surface renderings

Journal of Cell Science (2016) 129, 2250-2260 doi:10.1242/jcs.182592

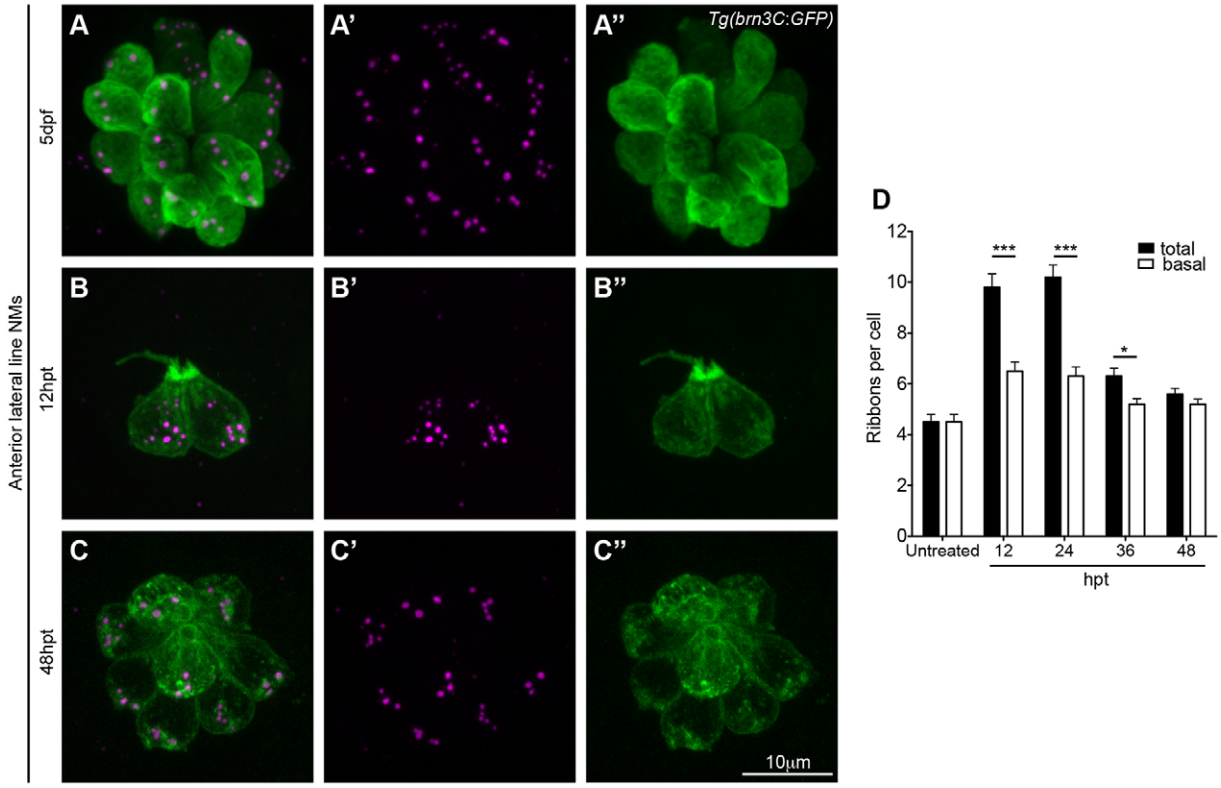

Fig. 5. Membrane-adjacent ribbons predominate in mature hair cells. (A–C″) 5 dpf *Tg(brn3C:GFP)* larvae were treated with 400 µM neomycin for 1 h to kill all hair cells. At different time points during regeneration larvae were fixed and stained with anti-GFP antibody (green, hair cells) and anti-RibeyeB antibody (magenta, ribbons), and three anterior lateral line neuromasts (NMs) (O2, MI1, MI2, IO4 or M2) were imaged using a confocal microscope. (D) Ribbons seen right next to the basal membrane in the green channel, as visualized in 3D surface renderings (Movies 6 and 7), were counted as basal ribbons, whereas the rest of the ribbons were considered as distal ribbons. At early time points during regeneration both distal ribbons and membrane adjacent ribbons were present in hair cells (12–36 hpt). Distal ribbons eventually disappeared, and by 48 h post treatment (hpt) ribbons adjacent to the basolateral membrane predominated. Ribbon numbers were obtained by visually counting ribbons in surface renderings of images of neuromasts (see Materials and Methods). Three neuromasts in three different larvae were imaged and ribbons were counted in a total of 26 hair cells of untreated larvae, 24 hair cells of 12 hpt larvae, 51 hair cells of 24 hpt larvae, 54 hair cells of 36 hpt larvae and 65 hair cells of 48 hpt larvae. *P=0.0124, ***P<0.0001 (unpaired two-tailed t-test). Results are mean±s.e.m.

of confocal images and rotating the renderings in 360° (Movies 5 and 6), we noticed that at earlier time points during regeneration [12–36 h post treatment (hpt)], ribbons, as detected by anti-RibeyeB antibody, were both distal from the basal membrane and adjacent to it (Fig. 5B–B″,D), although we do not have the resolution to distinguish between anchored ribbons and floating ribbons in proximity to the basal cell membrane. This ribbon phenotype was much like the one we observed in hair cells that lacked innervation. As hair cells matured, the number of ribbons decreased, particularly the number of the ribbons found distal to the basolateral membrane. By 48 h post treatment (hpt), membrane-adjacent ribbons predominated (Fig. 5C–C″,D; Movies 7 and 8), similar to the untreated controls (Fig. 5A–A"), again confirming that innervation is required for ribbon localization at the basolateral membrane.

TEM showed that early during regeneration, electron-dense structures were present in the cytoplasm (Fig. 6A–B′). We interpret these structures to be ribbon precursors, although immunoelectron microscopy for RibeyeB protein would be necessary to definitively prove their identity. Synaptic vesicles were often found near cytoplasmic ribbon precursors (Fig. 6A′). At different points during regeneration, we additionally found cases of double ribbons (Fig. 6C), ‘floating’ ribbons (i.e. ribbons not near a synapse) (Fig. 6E), ribbons next to what appear to be growth cones (Fig. 6G) and mature ribbons at synapses (Fig. 6D,F,H). Double ribbons and floating ribbons were rarely found at 72 hpt, after regenerated hair cells have matured (data not shown). Our observations of ribbon types at different time points during regeneration are summarized in Table S1.

Lack of mechanotransduction does not affect ribbon localization

Given that we show innervation to be important for ribbon regulation, we reasoned that mutants that lack hair cell mechanotransduction activity might also show defects in ribbon number, size and localization. To determine this, we assayed ribbons in *sputnik* mutants (*spu*) (Söllner et al., 2004), which lack mechanotransduction due to a mutation in *cadherin 23* that is required for tip-link formation between the stereocilia in hair cell bundles. By looking at ribbons in anterior lateral line hair cells (Fig. 7A–D′), we found that *spu* mutants had one fewer ribbon per hair cell when compared to their siblings (Fig. 7E), but the distribution of ribbon size did not seem different (Fig. 7B′,D′,F,G). Furthermore, ribbons appeared to be adjacent to the plasma membrane and not distal to it. This phenotype is very different from hair cells lacking innervation. We conclude that physical presence of afferent fibers is sufficient to regulate ribbon formation and stabilization.

DISCUSSION

Establishment of ribbon synapses in mechanosensory hair cells is imperative for their proper function. Our *in vivo* data of ribbons in

Journal of Cell Science (2016) 129, 2250-2260 doi:10.1242/jcs.182592

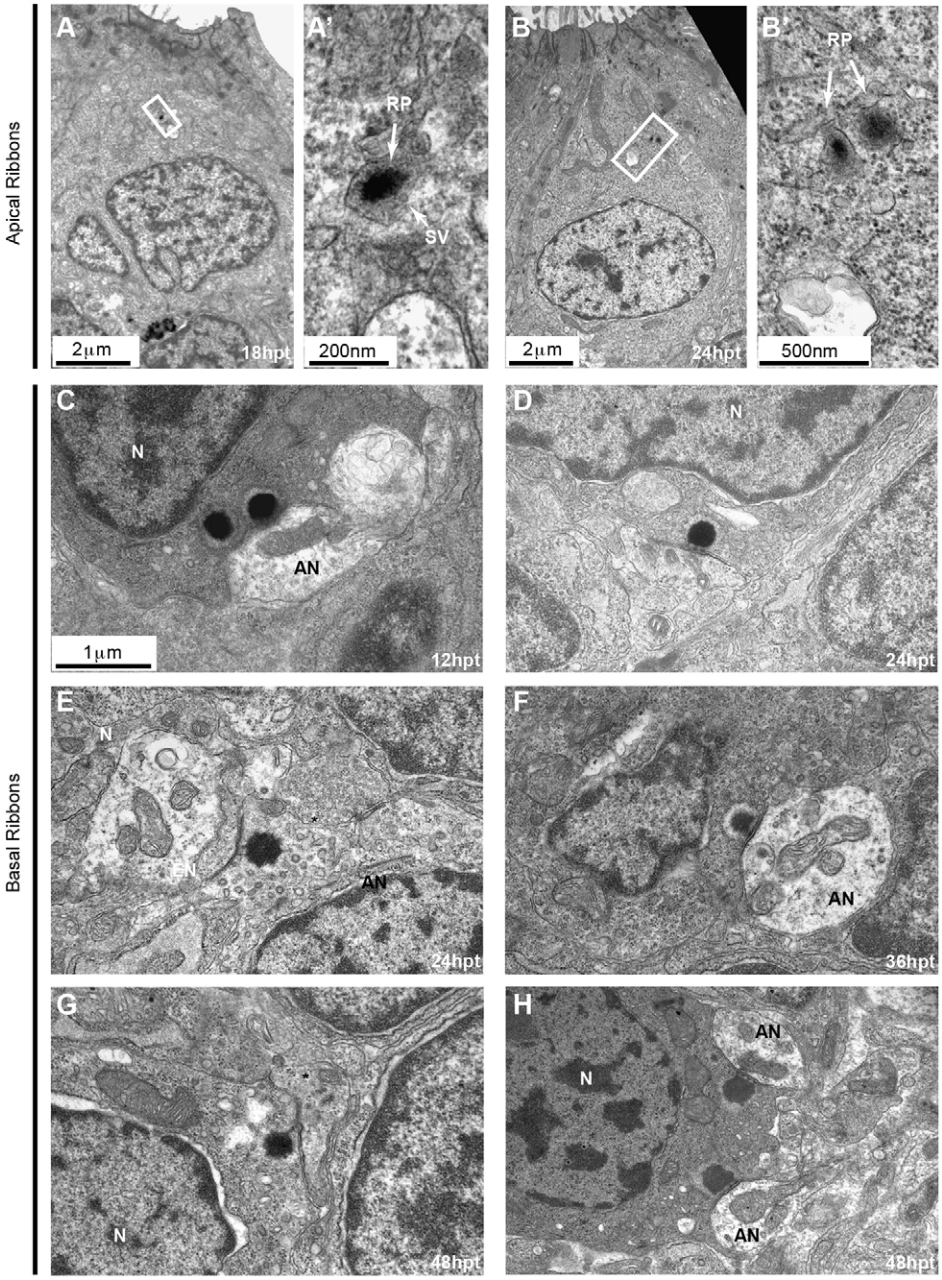

Fig. 6. Ultrastructural features of ribbons during hair cell regeneration. (A–I) 5 dpf larvae were treated with 400 µM neomycin for 1 h to kill all hair cells. To assess ribbon morphology during regeneration, larvae were fixed and processed for TEM and anterior lateral line neuromasts were imaged at different times post treatment (hpt). (A–B′) Electron-dense structures indicative of ribbon precursors are found in the cytoplasm of hair cells at early stages (18 hpt and 24 hpt) during regeneration. (A′,B′) Close up views of boxed regions in A,B. (C–H) Basal ribbons at different stages post treatment. Immature ribbons are seen at early stages such as double ribbons at 12 hpt (C) and 'ectopic' or 'floating' ribbons at 24 hpt (E) [the ribbon faces a support cell process (asterisk), which still separates the hair cell from a nearby afferent ending]. The immature ribbon anchored at the membrane at 48 hpt (G) faces a growth cone (asterisk), which has the characteristic dense cytoplasm filled with different size vesicles. Mature synapses (D,F,H) were clearly seen from 24 hpt to 48 hpt. N, nucleus; EN, efferent nerve ending; AN, afferent nerve ending. The images in D–H are shown at the same scale as that in C.

lateral line hair cells of *neurog1* mutant zebrafish that lack innervation show that ribbon generation is an intrinsic property of hair cells and occurs despite the absence of innervation. By contrast, analysis of ribbons in regenerating hair cells or ribbons in larvae where the innervating fibers have been transected shows that although innervation is not important for the initial ribbon formation, it influences ribbon number, size, localization and maintenance at the plasma membrane. These observations are consistent with prior observations of Puel and colleagues, who noticed ectopic or mislocalized synaptic bodies after the nerve endings were damaged by AMPA application in the cochlea (Puel et al., 1995) and with those of Sobkowicz and colleagues who showed mislocalization of ribbons at the plasma membrane in denervated cochlear cultures when compared to their innervated counterparts (Sobkowicz et al., 1986). How might innervating fibers regulate ribbon localization? Our hypothesis is that adhesion molecules that keep hair cells and their post-synaptic partners together also localize ribbons at the active zone juxtaposed to afferent fibers. This is perhaps accomplished indirectly through binding the cytomatrix protein Bassoon, because ribbons in *bassoon* mutants are found to be floating (Khimich et al., 2005; tom Dieck et al., 2005). As hair cells mature and synapses are formed, any ribbons that do not get localized at the membrane are likely degraded; therefore, we see a decrease in total ribbon number in mature hair cells during regeneration. Alternatively, the decrease of total ribbon number in mature hair cells might be due to the aggregation of several ribbon precursors, which also leads to bigger ribbons. When hair cells lose their innervation, ribbons lose their connection with the active zone, and perhaps even dissociate into smaller aggregates. These events would lead to an increase in ribbon number and decrease in overall ribbon size, as observed in specimens where the innervating fibers have been transected. Our hypothesis, therefore, is that ribbon localization at the synapse depends on contact of nerve fibers with hair cells and not on hair cell

Journal of Cell Science (2016) 129, 2250-2260 doi:10.1242/jcs.182592

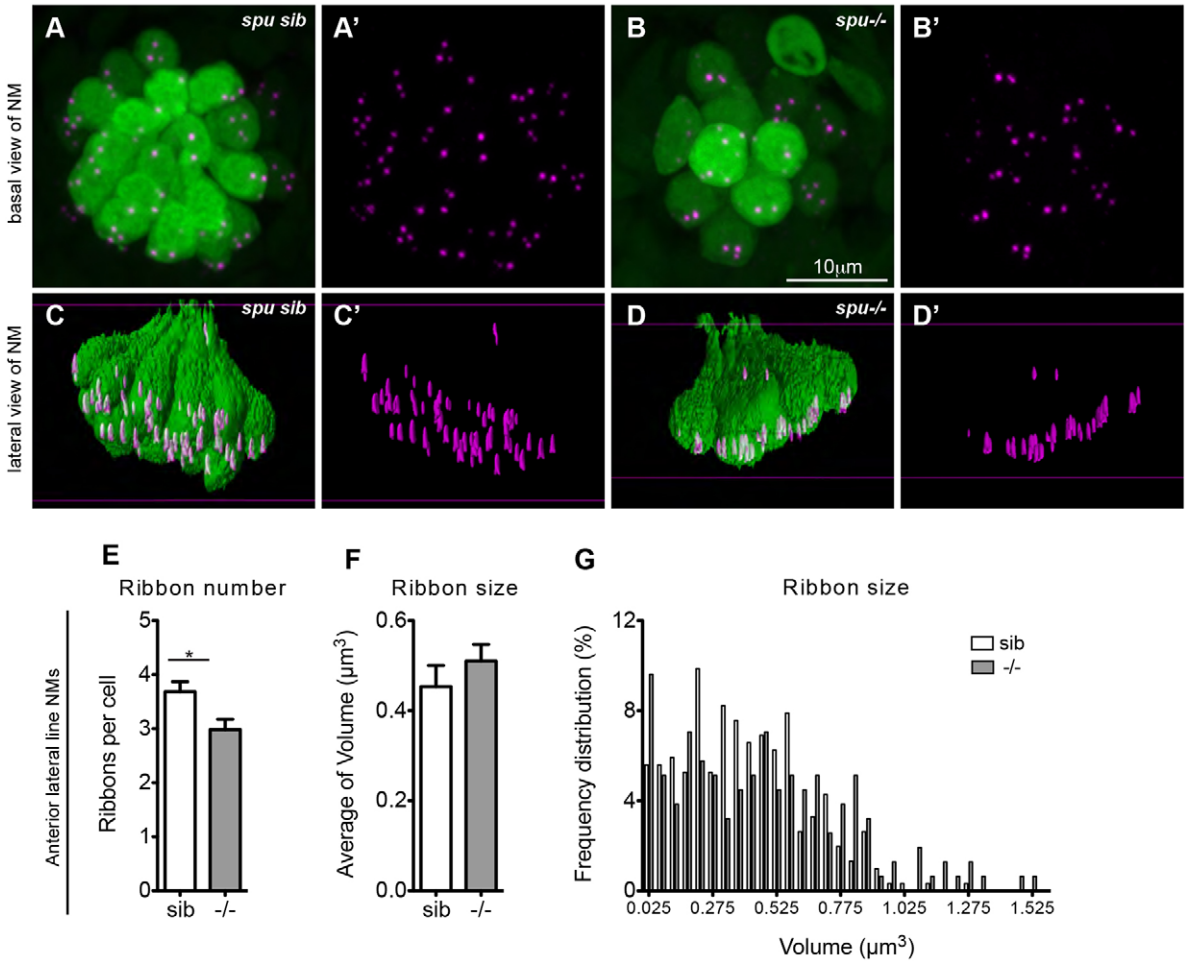

Fig. 7. Lack of mechanotransduction does not affect ribbon localization. (A–B′) *sputnik* (*spu*) siblings (sib) and mutants, which have a mutation in *cadherin 23* and lack tip links in their hair bundles, were fixed at 5 dpf and stained for hair cells (green, anti-parvalbumin antibody) and ribbons (magenta, anti-RibeyeB antibody). (A–B′) Projections of confocal images of anterior lateral line neuromasts (NM) (O2, MI1, MI2, IO4 or M2) in siblings and mutants. (C–D′) Lateral view of surface renderings of images in A–B′ generated by Huygens software. *spu* mutants had one less ribbon/cell (E), but ribbon size (F,G) and their localization (D′) was very similar to wild-type larvae. Ribbon size and number were obtained from the surface renderings of the neuromasts (see Materials and Methods). Statistical analysis of ribbons (unpaired two tailed *t*-test) was performed on averages of averages: average of ribbons, hair cells or neuromasts in a total of nine neuromasts (three neuromasts in three different larvae). Anterior lateral line neuromasts had an average of six hair cells per neuromast in *spu* mutant larvae and an average of 10 hair cells per neuromast in *spu* sibling larvae. **P*=0.02 (unpaired two-tailed *t*-test). The average ribbon size was not statistically different between mutants and their siblings, although the size as assessed by fluorescence microscopy is semi-quantitative. Results are mean±s.e.m.

activity. This theory is supported by our data in *spu* mutants that lack mechanotransduction, which show only a slight decrease in ribbon number and no changes in ribbon size. Similarly, another study shows that ribbon numbers do not change in *vglut3* zebrafish mutants, which fail to load glutamate in their synaptic vesicles (Obholzer et al., 2008). Interestingly, the presynaptic ribbon conversely plays a role on its post-synaptic partner, given that knocking down *ribeye* in zebrafish larvae leads to a decrease of afferent innervation (Sheets et al., 2011).

In conclusion, our work provides strong evidence that innervating fibers are crucial for regulating ribbon number, size and localization. Future studies will hopefully identify molecules that are important in this process.

MATERIALS AND METHODS

Zebrafish strains and husbandry

Zebrafish adults were maintained in our facility under standard conditions. The following transgenic and mutant zebrafish lines were used in our experiments: *Tg(brn3c:GFP)* (Xiao et al., 2005), *sputnik* (Söllner et al., 2004), *Tg(neurog1:EGFP)*^{w61} (McGraw et al., 2008), *neurog1 (neuroD3)*^{hi1089} mutant (Golling et al., 2002) and *Tg(neuroD:EGFP)* (Obholzer et al., 2008). To generate *neurog1* mutants and siblings for experiments in Fig. 2, double heterozygotes for *neurog1(neuroD3)*^{hi1089}; *Tg(neurog1:EGFP)*^{w61} were in-crossed. All mutants and siblings from this cross were selected for expression of the *neurog1:EGFP* transgene and subsequently processed for antibody staining. All animal experiments were performed according to approved IACUC protocols.

Immunohistochemistry and confocal microscopy

Standard immunohistochemistry techniques were used for antibody labeling (Suli et al., 2014). The following is the list of antibodies used for visualization: hair-cells, mouse anti-parvalbumin IgG1 (1:400, Millipore, MAB1572) with goat anti-mouse-IgG1 Alexa-Fluor-488-conjugated secondary (1:400, Invitrogen, A-21121); ribbons, rabbit anti-RibeyeB IgG (1:250) (Sheets et al., 2011) with goat anti-rabbit-IgG Alexa-Fluor-568-conjugated secondary antibody (1:400, Invitrogen, A-11011); afferent neurons, mouse anti-acetylated tubulin IgG2b (1:500, Sigma, T7451) with goat anti-mouse-IgG2b Alexa-Fluor-488-conjugated or goat anti-mouse-IgG2b Alexa-Fluor-633-conjugated secondary antibody

(1:400, Invitrogen, A-21146, A-21141); GFP, rabbit anti-GFP IgG (1:400, Invitrogen, A-11122) with goat anti-rabbit-IgG Alexa-Fluor-488-conjugated or goat anti-rabbit-IgG Alexa-Fluor-633 secondary antibody (1:400, Invitrogen, A-11008, A-21071).

Confocal fluorescent imaging stacks were acquired using an Olympus FV1000 confocal microscope. We used a UPLSAPO 60× water lens (NA:1.2), 6× zoom, 0.4–0.6 µm step size and resolution of 640×640 pixels/frame or 800×800 pixels/frame for image acquisition in Figs 2C–F′, 4C–F′, 5 and 7. For image acquisition in Figs 2A,B and 4A,B, we used a UPLSAPO20X air lens, NA 0.75, 1× zoom, 1.1 µm step size, resolution of 800×640 pixels/frame.

Transmission electron microscopy

Transmission electron microscopy (TEM) was performed in 2–7 days post fertilization (dpf) embryos and larvae as previously described (Owens et al., 2007). Briefly, zebrafish were euthanized in ice-cold embryo medium, fixed in ice-cold 4% glutaraldehyde in 0.1 M sodium cacodylate with 0.001% $CaCl_2$ (pH 7.4, 583 mOsm), washed with 0.1 M sodium cacodylate (pH 7.4) with 0.001% $CaCl_2$, post fixed in 1% osmium tetroxide in 0.1 M sodium cacodylate (pH 7.4) with $CaCl_2$, dehydrated in an ethanol series, washed in propylene oxide and then embedded in Spurr's epoxy resin in silicone rubber molds (Ted Pella, Redding, catalog no. 10504). After being baked at 60°C, blocks were cut to obtain sections from the anterior or posterior line neuromasts. Two series of ∼90-nm ultrathin sections separated by a 2-µm semi thin section were collected on 200 mesh Athene thin-gar grids (Ted Pella). The tissue was incubated in 5% uranyl acetate in 50% methanol, rinsed with 50% methanol and counterstained with 0.3% lead citrate in 0.1 N NaOH. The 2-µm semi-thin section between the series of ∼90-nm sections allowed observation of different hair cells within a neuromast. TEM was performed using a JEOL 1200EXII and a JEOL JEM 1400 microscopes. Although true serial sectioning was not performed, we followed the same ribbon in three to five sections on the same grid. For Figs 1 and 6, images were taken from the anterior lateral line neuromasts. For Fig. 3, ribbons were taken from the posterior lateral line neuromasts. Ribbon sizes in Fig. 1 were measured using ImageJ (see below).

Laser ablation

Tricaine (Sigma, E10521) anesthetized 5 dpf larvae were placed laterally in a Lab-Tek Chamber (Electron Microscopy Sciences, 70378-11) and overlaid with a fine nylon mesh and stainless steel harp for stabilization (Warner Instruments, 64-0253 SHD-26GH/10). Lateral line nerves anterior or at the level of the L1 neuromast were cut by exposure to three iterations of 5-ms 532-nm laser pulses (Ablate! System, Intelligent Imaging Innovations). Larvae were subsequently placed in fresh embryo medium and incubated at 28.5°C for 24 h before being processed for immunohistochemistry.

Live imaging

4 dpf *Tg(neuroD:EGFP)* transgenic larvae (Obholzer et al., 2008) were embedded sideways in 1% low-melting-point agarose (Sigma, A9414-10G) on glass bottom culture dishes (MatTek, P35G-0-10-C). 350×350 pixel/frame images were acquired using a Zeiss spinning disc microscope, with a 20× lens, 4× zoom, every 5 min for a total of 8 h. Using the same embedding and imaging set up, 5 dpf *Tg(neuroD:EGFP)* transgenic larvae were imaged every 5 min while being incubated in 400 µM neomycin for 1 h. After the incubation, neomycin was washed out. The larvae were re-embedded in fresh agarose and imaged every 5 min for another 12 h.

Data analysis

In Fig. 1, ImageJ was used to measure the diameter of ribbons in TEM sections from two or three larvae. Two measurements, one of the diameter perpendicular to the active zone and one of the diameter horizontal to the active zone, were collected for each ribbon. The two measurements were then averaged, and the averages for each ribbon were graphed using GraphPad.

SVI Huygens software was used to analyze confocal image stacks. The images were deconvolved, cropped to 480×480 pixels and the advanced object analyzer was used to generate surface renderings and measure the size and number of each ribbon. In an effort to standardize the image processing, fixed threshold settings were applied to all the images, but that failed to sometimes capture all the ribbons. As a result, for each image the best fitting threshold was set to capture all the ribbons. To find whether experimentalist-determined threshold settings gave reproducible results, the same image was processed two different times, which included setting thresholds and measuring the objects. The two different datasets obtained this way were not statistically significantly different from one another; hence, we manually set the thresholds each time. To determine the number of ribbons per cell in *neurog1* and *spu* mutant and sibling larvae (Figs 2 and 7) confocal images of hair cells in three neuromasts of three different larvae were deconvolved and surface renderings were generated using Huygens. A region-of-interest (ROI) sphere was fitted to the base of each hair cell (green channel) in a given neuromast. Following that, the number of ribbons, size and ribbon *x-y* coordinates within each sphere (hair cell) were collected in the red channel. The inter-ribbon distance was then calculated as the Euclidian distance between coordinates using the Matlab *pdist* function. The average ribbon size and number was calculated for each neuromast using Microsoft Excel, and the data was subsequently entered in GraphPad software to generate graphs and for statistical analysis.

In Fig. 4, images of hair cells of three neuromasts in two different larvae were acquired for each of the uncut and cut conditions. Using Huygens software, the images were deconvolved, surface renderings were generated and the ribbon size and number per neuromast was collected. In this experiment, we did not use the ROI method to obtain the number of ribbons per hair cell. Instead ribbon number and size was obtained at the neuromast level and the number of ribbons per hair cell was calculated as a ratio of total ribbons to the number of hair cells in the neuromast. The average ribbon size and number was calculated in Microsoft Excel. The data was then graphed and statistical analysis was performed using GraphPad.

In Fig. 5, images of hair cells of three neuromasts in three different larvae were acquired using Olympus FV1000, deconvolved using Huygens and the ribbon number per each hair cell in each neuromast was visually counted from images in 3D surface renderings. Any ribbon that in 3D surface renderings was right next to the cell membrane was designated as basal. The average ribbon number per neuromast was generated in Microsoft Excel and the data was graphed in GraphPad.

Acknowledgements

We thank Steve MacFarlane in the Electron Microscopy Resource Center at University of Washington for sectioning electron microscopy samples, David White in the Zebrafish Facility at University of Washington for fish care and maintenance, Teresa Nicolson at OHSU (Portland, OR) for providing us with anti-RibeyeB antibody and *sputnik* mutants, Heather Brignull and Michael Stark for editing the manuscript.

Competing interests

The authors declare no competing or financial interests.

Author contributions

A.S. designed and performed experiments, analyzed data, wrote the manuscript; R.P. designed and performed experiments, analyzed data, edited manuscript; D.E.C. performed experiments; D.W.H. performed experiments, edited manuscript; A.P. analyzed data, edited manuscript; E.W.R. designed experiments, edited manuscript; D.W.R. designed experiments, edited manuscript.

Funding

This work was supported by the Hearing Health Foundation (grant to A.S.); the National Institute on Deafness and Other Communication Disorders [grant numbers T32 DC000018-28 to A.S., R01DC005987 to D.W.R. and E.W.R., R01DC011269 to D.W.R.]. The Bloedel Visitor Scholar Program funded most of the work of R.P. in Seattle. Deposited in PMC for release after 12 months.

Supplementary information

Supplementary information available online at
http://jcs.biologists.org/lookup/suppl/doi:10.1242/jcs.182592/-/DC1

References

Baker, C. F. and Montgomery, C. J. (1999). The sensory basis of rheotaxis in the blind Mexican cave fish, *Astyanax fasciatus*. *J. Comp. Physiol. A* **184**, 519-527.

Blanks, J. C., Adinolfi, A. M. and Lolley, R. N. (1974). Synaptogenesis in the photoreceptor terminal of the mouse retina. *J. Comp. Neurol.* **156**, 81-93.

Blaxter, J. H. S. and Fuiman, L. A. (1989). Function of the free neuromasts of marine teleost larvae. In *The Mechanosensory Lateral Line: Neurobiology and Evolution* (eds S. Coombs et al.), pp. 482-499. New York: Springer-Verlag.

Brandstatter, J. H., Fletcher, E. L., Garner, C. C., Gundelfinger, E. D. and Wassle, H. (1999). Differential expression of the presynaptic cytomatrix protein bassoon among ribbon synapses in the mammalian retina. *Eur. J. Neurosci.* **11**, 3683-3693.

Brandt, A., Striessnig, J. and Moser, T. (2003). CaV1.3 channels are essential for development and presynaptic activity of cochlear inner hair cells. *J. Neurosci.* **23**, 10832-10840.

Buran, B. N., Strenzke, N., Neef, A., Gundelfinger, E. D., Moser, T. and Liberman, M. C. (2010). Onset coding is degraded in auditory nerve fibers from mutant mice lacking synaptic ribbons. *J. Neurosci.* **30**, 7587-7597.

Dick, O., tom Dieck, S., Altrock, W. D., Ammermuller, J., Weiler, R., Garner, C. C., Gundelfinger, E. D. and Brandstatter, J. H. (2003). The presynaptic active zone protein bassoon is essential for photoreceptor ribbon synapse formation in the retina. *Neuron.* **37**, 775-786.

Dijkgraaf, S. (1963). The functioning and significance of the lateral-line organs. *Biol. Rev. Camb. Philos. Soc.* **38**, 51-105.

Dijkgraaf, S. (1989). A short personal review of the history. In *The Mechanosensory Lateral Line: Neurobiology and Evolution* (eds S. Coombs et al.), pp. 7-13. New York: Springer-Verlag.

Dou, H., Vazquez, A. E., Namkung, Y., Chu, H., Cardell, E. L., Nie, L., Parson, S., Shin, H.-S. and Yamoah, E. N. (2004). Null mutation of alpha1D Ca2+ channel gene results in deafness but no vestibular defect in mice. *J. Assoc. Res. Otolaryngol.* **5**, 215-226.

Ghysen, A. and Dambly-Chaudiere, C. (2007). The lateral line microcosmos. *Genes Dev.* **21**, 2118-2130.

Golling, G., Amsterdam, A., Sun, Z., Antonelli, M., Maldonado, E., Chen, W., Burgess, S., Haldi, M., Artzt, K., Farrington, S. et al. (2002). Insertional mutagenesis in zebrafish rapidly identifies genes essential for early vertebrate development. *Nat. Genet.* **31**, 135-140.

Grant, K. A., Raible, D. W. and Piotrowski, T. (2005). Regulation of latent sensory hair cell precursors by glia in the zebrafish lateral line. *Neuron* **45**, 69-80.

Harris, J. A., Cheng, A. G., Cunningham, L. L., MacDonald, G., Raible, D. W. and Rubel, E. W. (2003). Neomycin-induced hair cell death and rapid regeneration in the lateral line of zebrafish (Danio rerio). *J. Assoc. Res. Otolaryngol.* **4**, 219-234.

Hassan, E. S. (1989). Hydrodynamic imaging of the surroundings by the lateral line of the blind cave fish Anoptichthys jordani. In *The Mechanosensory Lateral Line: Neurobiology and Evolution* (eds S. Coombs et al.) New York: Springer-Verlag.

Hoekstra, D. and Janssen, J. (1985). Non-visual feeding behavior of the mottled sculpin, *Cottus bairdi*, in Lake Michigan. *Environ. Biol. Fish* **12**, 111-117.

Kalmijn, A. D. (1989). Function evolution of lateral line and inner ear sensory systems. In *The Mechanosensory Lateral Line* (eds S. Coombs, P. Gorner and H. Munz), pp. 187-215. New York: Springer-Verlag.

Kanter, M. J. and Coombs, S. (2003). Rheotaxis and prey detection in uniform currents by Lake Michigan mottled sculpin (Cottus bairdi). *J. Exp. Biol.* **206**, 59-70.

Khimich, D., Nouvian, R., Pujol, R., Tom Dieck, S., Egner, A., Gundelfinger, E. D. and Moser, T. (2005). Hair cell synaptic ribbons are essential for synchronous auditory signalling. *Nature* **434**, 889-894.

Magupalli, V. G., Schwarz, K., Alpadi, K., Natarajan, S., Seigel, G. M. and Schmitz, F. (2008). Multiple RIBEYE-RIBEYE interactions create a dynamic scaffold for the formation of synaptic ribbons. *J. Neurosci.* **28**, 7954-7967.

Matthews, G. and Fuchs, P. (2010). The diverse roles of ribbon synapses in sensory neurotransmission. *Nat. Rev. Neurosci.* **11**, 812-822.

Maxeiner, S., Luo, F., Tan, A., Schmitz, F. and Sudhof, T. C. (2016). How to make a synaptic ribbon: RIBEYE deletion abolishes ribbons in retinal synapses and disrupts neurotransmitter release. *EMBO J.* **35**, 793-899.

McGraw, H. F., Nechiporuk, A. and Raible, D. W. (2008). Zebrafish dorsal root ganglia neural precursor cells adopt a glial fate in the absence of neurogenin1. *J. Neurosci.* **28**, 12558-12569.

Montgomery, J. C. and Hamilton, A. R. (1997). Sensory contributions to nocturnal prey capture in the dwarf scorpion fish (*Scorpaena papillosus*). *Mar. Freshwater Behav. Physiol.* **30**, 209-223.

Montgomery, J. C., Baker, C. F. and Carton, A. G. (1997). The lateral line can mediate rheotaxis in fish. *Nature* **389**, 960-963.

Moser, T., Brandt, A. and Lysakowski, A. (2006). Hair cell ribbon synapses. *Cell Tissue Res.* **326**, 347-359.

Nicolson, T. (2005). The genetics of hearing and balance in zebrafish. *Annu. Rev. Genet.* **39**, 9-22.

Nicolson, T. (2015). Ribbon synapses in zebrafish hair cells. *Hear. Res.* **330**, 170-177.

Nicolson, T., Rüsch, A., Friedrich, R. W., Granato, M., Ruppersberg, J. P. and Nüsslein-Volhard, C. (1998). Genetic analysis of vertebrate sensory hair cell mechanosensation: the zebrafish circler mutants. *Neuron* **20**, 271-283.

Nouvian, R., Beutner, D., Parsons, T. D. and Moser, T. (2006). Structure and function of the hair cell ribbon synapse. *J. Membr. Biol.* **209**, 153-165.

Obholzer, N., Wolfson, S., Trapani, J. G., Mo, W., Nechiporuk, A., Busch-Nentwich, E., Seiler, C., Sidi, S., Söllner, C., Duncan, R. N. et al. (2008). Vesicular glutamate transporter 3 is required for synaptic transmission in zebrafish hair cells. *J. Neurosci.* **28**, 2110-2118.

Owens, K. N., Cunningham, D. E., MacDonald, G., Rubel, E. W., Raible, D. W. and Pujol, R. (2007). Ultrastructural analysis of aminoglycoside-induced hair cell death in the zebrafish lateral line reveals an early mitochondrial response. *J. Comp. Neurol.* **502**, 522-543.

Platzer, J., Engel, J., Schrott-Fischer, A., Stephan, K., Bova, S., Chen, H., Zheng, H. and Striessnig, J. (2000). Congenital deafness and sinoatrial node dysfunction in mice lacking class D L-type Ca2+ channels. *Cell* **102**, 89-97.

Puel, J. L., Saffiedine, S., Gervais d'Aldin, C., Eybalin, M. and Pujol, R. (1995). Synaptic regeneration and functional recovery after excitotoxic injury in the guinea pig cochlea. *C. R. Acad. Sci. III* **318**, 67-75.

Pujol, R., Lavigne-Rebillard, M. and Lenoir, M. (1997). Development of sensory and neural structures in the mammalian cochlea. In *Development of Sensory Auditory System* (ed. E. W. Rubel, A. N. Popper. and R. R. Fay), pp. 146-192. New York: Springer.

Pujol, R., Carlier, E. and Devigne, C. (1979). Significance of presynaptic formations in early stages of cochlear synaptogenesis. *Neurosci. Lett.* 15, 97-102.

Raible, D. W. and Kruse, G. J. (2000). Organization of the lateral line system in embryonic zebrafish. *J. Comp. Neurol.* **421**, 189-198.

Regus-Leidig, H., Tom Dieck, S., Specht, D., Meyer, L. and Brandstätter, J. H. (2009). Early steps in the assembly of photoreceptor ribbon synapses in the mouse retina: the involvement of precursor spheres. *J. Comp. Neurol.* **512**, 814-824.

Schmitz, F., Königstorfer, A. and Südhof, T. C. (2000). RIBEYE, a component of synaptic ribbons: a protein's journey through evolution provides insight into synaptic ribbon function. *Neuron* **28**, 857-872.

Sheets, L., Trapani, J. G., Mo, W., Obholzer, N. and Nicolson, T. (2011). Ribeye is required for presynaptic Ca(V)1.3a channel localization and afferent innervation of sensory hair cells. *Development* **138**, 1309-1319.

Sheets, L., Kindt, K. S. and Nicolson, T. (2012). Presynaptic CaV1.3 channels regulate synaptic ribbon size and are required for synaptic maintenance in sensory hair cells. *J. Neurosci* **32**, 17273-17286.

Sidi, S., Busch-Nentwich, E., Friedrich, R., Schoenberger, U. and Nicolson, T. (2004). gemini encodes a zebrafish L-type calcium channel that localizes at sensory hair cell ribbon synapses. *J. Neurosci.* **24**, 4213-4223.

Sobkowicz, H. M., Rose, J. E., Scott, G. E. and Slapnick, S. M. (1982). Ribbon synapses in the developing intact and cultured organ of Corti in the mouse. *J. Neurosci.* **2**, 942-957.

Sobkowicz, H. M., Rose, J. E., Scott, G. L. and Levenick, C. V. (1986). Distribution of synaptic ribbons in the developing organ of Corti. *J. Neurocytol.* **15**, 693-714.

Söllner, C., Rauch, G.-J., Siemens, J., Geisler, R., Schuster, S. C., Müller, U., Nicolson, T. and Tübingen Screen, C. (2004). Mutations in cadherin 23 affect tip links in zebrafish sensory hair cells. *Nature* **428**, 955-959.

Sterling, P. and Matthews, G. (2005). Structure and function of ribbon synapses. *Trends Neurosci.* **28**, 20-29.

Suli, A., Watson, G. M., Rubel, E. W. and Raible, D. W. (2012). Rheotaxis in larval zebrafish is mediated by lateral line mechanosensory hair cells. *PLoS ONE* **7**, e29727.

Suli, A., Guler, A. D., Raible, D. W. and Kimelman, D. (2014). A targeted gene expression system using the tryptophan repressor in zebrafish shows no silencing in subsequent generations. *Development* **141**, 1167-1174.

tom Dieck, S., Altrock, W. D., Kessels, M. M., Qualmann, B., Regus, H., Brauner, D., Fejtová, A., Bracko, O., Gundelfinger, E. D. and Brandstätter, J. H. (2005). Molecular dissection of the photoreceptor ribbon synapse: physical interaction of Bassoon and RIBEYE is essential for the assembly of the ribbon complex. *J. Cell Biol.* **168**, 825-836.

Wan, L., Almers, W. and Chen, W. (2005). Two ribeye genes in teleosts: the role of Ribeye in ribbon formation and bipolar cell development. *J. Neurosci.* **25**, 941-949.

Webb, J. F. and Shirey, J. E. (2003). Postembryonic development of the cranial lateral line canals and neuromasts in zebrafish. *Dev. Dyn.* **228**, 370-385.

Wong, A. B., Rutherford, M. A., Gabrielaitis, M., Pangršič, T., Göttfert, F., Frank, T., Michanski, S., Hell, S., Wolf, F., Wichmann, C. et al. (2014). Developmental refinement of hair cell synapses tightens the coupling of Ca2+ influx to exocytosis. *EMBO J.* **33**, 247-264.

Xiao, T., Roeser, T., Staub, W. and Baier, H. (2005). A GFP-based genetic screen reveals mutations that disrupt the architecture of the zebrafish retinotectal projection. *Development* **132**, 2955-2967.

Yu, W.-M. and Goodrich, L. V. (2014). Morphological and physiological development of auditory synapses. *Hear. Res.* **311**, 3-16.

Yu, W.-M., Appler, J. M., Kim, Y.-H., Nishitani, A. M., Holt, J. R. and Goodrich, L. V. (2013). A Gata3-Mafb transcriptional network directs post-synaptic differentiation in synapses specialized for hearing. *Elife* **2**, e01341.

Yuan, Y. and Chi, F. (2014). Dynamic changes in hair cell ribbon synapse induced by loss of spiral ganglion neurons in mice. *Chin. Med. J.* **127**, 1941-1946.
Zenisek, D., Horst, N. K., Merrifield, C., Sterling, P. and Matthews, G. (2004). Visualizing synaptic ribbons in the living cell. *J. Neurosci.* **24**, 9752-9759.
Zuccotti, A., Kuhn, S., Johnson, S. L., Franz, C., Singer, W., Hecker, D., Geisler, H.-S., Kopschall, I., Rohbock, K., Gutsche, K. et al. (2012). Lack of brain-derived neurotrophic factor hampers inner hair cell synapse physiology, but protects against noise-induced hearing loss. *J. Neurosci.* **32**, 8545-8553.